IOP Publishing

An Introduction to Photonics and Laser Physics with Applications

Prem B Bisht

Chapter 24

Coherent radiation obtained using special geometries

Summary: In this book we have discussed the principles and properties of some of the lasers and other coherent light sources given in the following table (table 24.1). Details of various lasers covering the broad region of the UV–visible–IR spectrum are summarized in the table. Coherent radiation produced using nonlinear optics techniques such as second-harmonic generation/third-harmonic generation (SHG/THG) and optical parametric amplifiers/optical parametric oscillators (OPAs/OPOs) contribute to this; hence, it is by no means an exhaustive list. In this chapter, the principles of a few special types of laser and an up-to-date laser technology, viz. the generation of laser pulses on the attosecond timescale (10^{-18}s) as well as laser power levels of petawatts (10^{15}W) are discussed. Among the techniques described here are (i) the mirrorless distributed feedback (DFB) laser, (ii) the free-electron laser (FEL), and (iii) high harmonic generation (HHG) and soft x-ray lasers.

Learning objectives

After reading this chapter, the learner will be able to:

List the gas, solid, and liquid lasers;
Identify the lasers used to obtain light in various regions of the electromagnetic (EM) spectrum;
Understand the principle of mirrorless lasers;
Identify light sources based on the acceleration of electrons;
Explain the principle of the FEL;
Describe the mechanism of HHG;
Confirm that attosecond pulses can be generated in the deep-UV/x-ray region;
Summarize the future outlook of lasers.

doi:10.1088/978-0-7503-5226-0ch24

Table 24.1. The gain media, pumping mechanisms, and output wavelengths of some of the lasers and coherent radiations referred to in this book.

S. No.	Source of coherent radiation	Gain-medium type and (pumping*)	Gain medium	Major wavelengths	Chapter no.
1	He–Ne laser	Gas (Elect)	He:Ne (8:1)	626.8, 543.5 nm	6
2	Argon laser	Gas (Elect)	Argon gas	514.5, 488 nm	6
3	Nitrogen laser	Gas (Elect)	Air/nitrogen gas	336 nm	7
4	Excimer laser	Gas (Elect)	XeCl	308 nm	
5	CO_2 laser	Gas (Elect)	CO_2	9.4, 10.6 μm	6
6	Dye laser	Liquid (Opt)	Dyes	Near UV–VIS–near IR	2
7	Nd:YAG laser	Solid (Opt)	Nd^{+3} in YAG	1064 nm	6
8	Nd: Glass laser	Solid (Opt)	Nd^{+3} in glass	1050 nm	8
9	Ti:sapphire laser	Solid (Opt)	$Ti^{+3:}$: Al_2O_3	750–1100 nm	20
10	Ruby laser	Solid (Elect)	$Cr^{+3:}$ Al_2O_3	694.3 nm	
11	Diode laser	Solid (Elect)	Semiconductors	Various	22
12	Quantum cascade laser	Solid (Elect)	Quantum wells, electrons	Tunable in IR	22
13	OPO/OPA	Solid (Opt)	NLO crystals	Tunable in VIS/IR	16
14	Fiber laser	Solid (Opt)	SiO_2 (Glass)	1550 nm region	23
15	EDFA	Solid (Opt)	Er^{+3} in fibers	1550 nm	23
16	DFB laser	Solid, liquid (Opt, elect)	Semiconductors/dyes	Tunable in VIS	22
17	FEL	Gas/(Elect)	Accelerated electrons	Tunable	24
18	Raman laser	Solid/liquid/gas (Opt)	Several materials	Several	24
19	EUV and x-ray lasers	Gas/solid (Opt)	Argon, other gases	Soft x-ray	24
20	VCSEL	Solid (Elect)	Semiconductors	Various	22
21	F8L	Solid	Er^{+3} doped fiber	1550 nm	23

* Elect: electrical pumping, Opt: optical pumping, EDFA: erbium-doped fiber amplifier, EUV: extreme UV, VCSEL: vertical-cavity surface-emitting laser, F8L: figure-of-eight laser, YAG: yttrium aluminum garnet, NLO: nonlinear optics, VIS: visible

24.1 Mirrorless laser cavities

In conventional lasers, the two cavity mirrors provide the feedback necessary for laser oscillation. In distributed feedback (DFB) lasers, there are no mirrors. Here, the spatially periodic structure in the gain medium not only gives the necessary feedback for the oscillation but also provides the mechanism that restricts the oscillation to a narrow frequency range. Their compact design, mechanical stability, fine frequency tunability, and ultrafast pulse generation capability make DFB lasers versatile and indispensable. The principle of DFB is used in several applications in photonics.

24.1.1 Principle of DFB lasers

Laser oscillation can be generated by incorporating a periodic, grating-like structure in the gain medium. The grating-like structure is obtained either by direct interference methods or by inscribing a permanent grating at the required spacing using lithographic techniques. In direct interference methods, two replica beams of a pump laser (focused by a cylindrical lens to prepare light-sheets) can interfere in an absorbing medium as shown in figure 24.1. Due to interference and the absorption of light, a grating-like structure is formed in the medium (figure 24.2).

♣ In the lithographic technique, micro-fabricated patterns are transferred from a prefabricated photo-sensitive mask onto the substrate. Excimer lasers with pulses in the far UV region are used to create the minimum features.

The periodicity of the spatial modulation (Λ) or the fringe spacing is determined by the half angle ($\theta/2$) between the two interfering beams as follows:

$$\Lambda = \lambda_{\text{pump}}/2 \sin(\theta/2) \tag{24.1}$$

where λ_{pump} is the wavelength of the pump laser. A light wave undergoes Bragg reflection at this periodical structure, which provides the feedback necessary for laser action (figure 24.2).

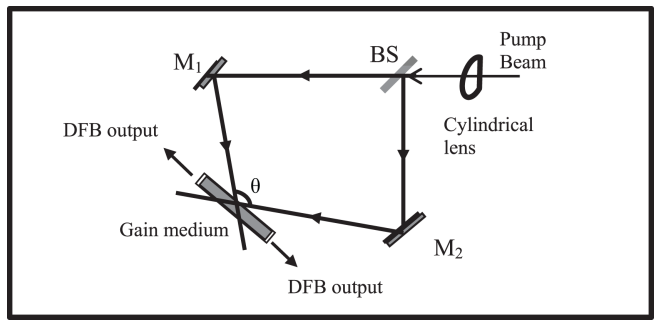

Figure 24.1. Typical setup for a distributed feedback laser. M1, M2: mirrors, B.S: beam splitter. The interference region at the gain medium is shown on an expanded scale in figure 24.2.

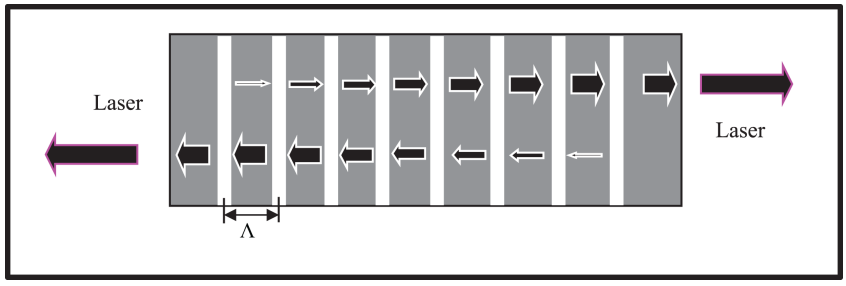

Figure 24.2. Increase of laser photons in a DFB laser. The interference fringes (i.e. the grating) are shown as white stripes. The thicknesses of the arrows indicate the amplification of light along the length of the gain medium.

In DFB lasers the feedback is provided by backward Bragg scattering from the spatially periodic modulation of the laser medium. Due to Bragg-angle dependence, the feedback is strongly frequency selective and the resonant mode for laser oscillation corresponds to the wavelength (λ_{DFB}) that satisfies Bragg's law for various orders (m).

$$\lambda_{\mathrm{DFB}} = \frac{n\lambda_{\mathrm{pump}}}{m \sin(\theta/2)}$$

Here, n is the refractive index of the gain medium. Finally, only photons with wavelengths that can propagate along the length of the gain medium are responsible for amplification (figure 24.2) . Hence, the equation for the *first order* can be rewritten as

$$\lambda_{\mathrm{DFB}} = 2n\Lambda \tag{24.2}$$

Equation (24.2) shows that the laser can be tuned by varying the refractive index or the intersection angle that decides the fringe spacing.

The stimulated emission in the distributed gain medium gives rise to two counter-running waves. The total field (E) in the medium is the sum of these waves (figure 24.3) with complex amplitudes $R(z)$ and $S(z)$ respectively, as follows:

$$E = R(z)\mathrm{e}^{-\mathrm{ikz}/2} + S(z)\mathrm{e}^{\mathrm{ikz}/2}. \tag{24.3}$$

where $k = 2\pi/\Lambda$. These two waves experience gains as they travel in the population-inverted region through the gain medium. The inversion builds up due to pump photons until the field increases sufficiently for gain saturation to become dominant. At this moment, the Bragg reflectivity decreases rapidly, allowing the field to escape as a beam with a narrow linewidth restricted according to equation (24.2).

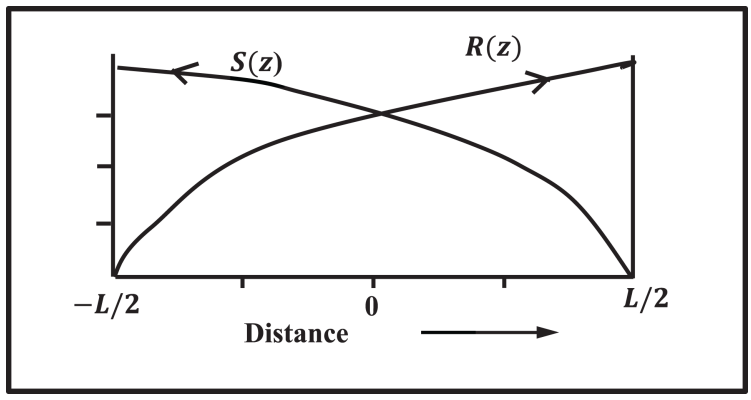

Figure 24.3. Spatial dependence of the amplitudes of the counter-propagating waves ($R(z)$ and $S(z)$) in a gain medium of length (L).

24.1.2 Ultrashort pulses and the tunability of DFB lasers

DFB lasers are used to generate short-duration pulses from longer ones. DFB lasers are also capable of fine-tuning laser frequencies of the order of 1 KHz or even less due to Bragg selectivity. DFB techniques have been applied to dye lasers and semiconductor lasers. If dye is used as a gain medium, the resulting laser is known as the distributed feedback dye laser (DFDL). Short pulses can be obtained on pumping with pulsed lasers due to the self-Q-switching effect. Self-Q-switching derives its name from the effect of saturable absorption as described in chapter 17. When the energy stored in the gain medium overcomes the losses and can then be transmitted in the form of an optical pulse, this is known as self-Q-switching. If this occurs in gain-coupled pulsed DFB lasers, the self-Q switching mechanism leads to transform-limited pulses that are shorter than the pump pulse by a factor of 50–100.

24.2 Coherent radiation based on acceleration of charge

An oscillating charge behaves like a dipole that radiates in the manner described in section 1.4.4. Here, we will describe two kinds of laser based on this principle, albeit in entirely different contexts. The first is the FEL, while the second is based on the phenomenon of HHG.

24.2.1 Free-electron lasers

As outlined in section 1.4.4, an accelerating charge near the speed of light gives rise to EM radiation. The power of this radiation is proportional to the square of the acceleration of the charge. As shown schematically in figure 24.4, in FEL, an array of alternating magnetic fields in the form of a grating structure is built to oscillate the charge. The strengths of the magnetic fields are of the order of 0.01–1 T. The electrons are sent into this magnetic field at relativistic speeds to oscillate in vacuum. In this configuration, electron beam energies of the order of gigaelectron volts are used.

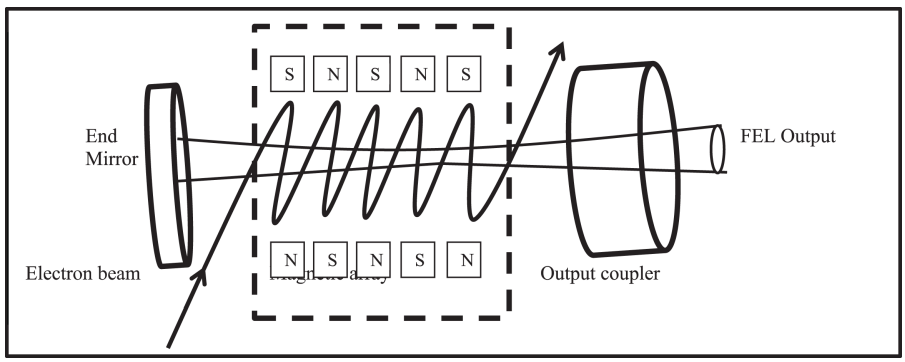

Figure 24.4. Schematic diagram of a free-electron laser (FEL). N and S are the magnetic poles. The electron beam enters the magnetic array and exits from the cavity as indicated by arrows.

The radiation predominantly propagates in the direction perpendicular to the dipole vector. As we know, in conventional lasers such as the He–Ne laser, the laser's output wavelength is decided by the discrete transition frequencies of the gain media. In contrast, in FELs, the lasing wavelength is decided by the kinetic energy of the oscillating electrons passing through an array of magnetic structures. Hence, the laser frequencies result from transitions between continuous states. As a result, the FEL is a coherent light source with wide wavelength tunability, especially in the far-IR region.

Depending on the length as well as the strength of the magnetic array, a large spectral range of wavelengths from nanometers (the x-ray region) to a few tens of millimeters (in the microwave range) can be obtained. The nature of the electron beam used in an FEL selects either pulsed or continuous-wave operation. The output powers of various FELs can be in the gigawatt range for pulsed operation. The source of electrons can be a storage ring or a linear accelerator similar to those used in synchrotron sources.

♣ In synchrotron sources the radiation obtained can be monochromatic but not coherent. Using FELs, due to fast interactions, the micro bunching of electrons, and Compton scattering (♠ see section 2.8), coherent monochromatic radiation is obtained.

Figure 24.4 shows a schematic of an FEL, in which the cavity mirrors are placed in the perpendicular direction to that of the oscillating electrons. The high-energy electrons are prevented from hitting the mirrors by magnetic reflectors. The radiation traveling between the mirrors is amplified at the desired frequency, which is set by the speed and the grating period of the magnetic array.

24.2.2 Extreme UV and soft x-ray lasers

Figure 24.5 gives an expanded view of figure 2.1 in the vacuum UV (10 eV) to hard x-ray (10 keV) region. It should be noted that the photons of vacuum ultraviolet (VUV) can be absorbed by less than 1 mm of air and are able to ionize several substances. All materials are ionized by extreme UV (EUV) radiation. Soft x-rays interact with the core electrons of materials. The wavelengths of hard x-rays fall

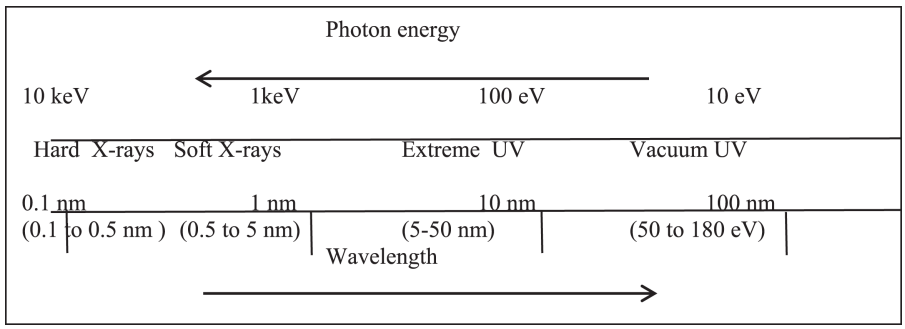

Figure 24.5. Expanded version of figure 2.1 in the deep-UV and x-ray regions.

within the size range of the lattice spacings of crystals, which is the reason why x-ray sources are used for the determination of crystal structure.

EUV is an emerging research field in the scientific and technological applications of photonics. Therefore, we will now learn about two methods used to obtain radiation in the EUV and soft x-ray region using conventional lasers. These methods fall under the category of HHG and use the principles of (i) the tunnel ionization and recombination process, and (ii) the cascading Raman scattering process.

24.2.2.1 The Keldysh parameter and the HHG process

As described in chapter 16, most of the perturbative-type nonlinear optical phenomena are described by equation 16.6. However, if the electric field strength is greater than the Coulomb field of the atom, the effects of perturbative-type nonlinearity are no longer manifested, due to a new type of atom–field interaction. In such cases, incident field-induced tunneling of electrons takes place through the atomic potential. Following the Lorentz-Drude model of the atom, the atomic field strength is given by $E_{\text{atomic}} \sim \text{m}^{-1}$ (♠ see section 14.2.1). For larger incident fields, a new dimensionless adiabaticity parameter known as the Keldysh parameter (γ) needs to be introduced. This parameter helps us to identify the two regions of nonlinear optics. It is defined as the ratio between the laser-field frequency (ω) and the tunneling frequency (ω_t). Therefore, γ relates the strength of the laser field and the ionization potential of the atom.

For free electrons generated by high field interactions, the values of the electric fields generated by lasers fall in the intensity range of the order of $>10^{16}$ W cm^{-2}. Lasers can produce fields several orders higher than such values. As indicated in figure 24.6, the effects at these high energies do not fall under the perturbative approach of quantum mechanics. A detailed description of such effects is outside the scope of this textbook. Briefly, a new approach to nonlinear optics has to be considered for a free electron in an intense laser field, as follows.

The time-averaged kinetic energy associated with the motion of a free electron (of charge q and mass m) in an electric field E with frequency ω is given by

$$K = \frac{q^2E^2}{m\omega^2}.$$

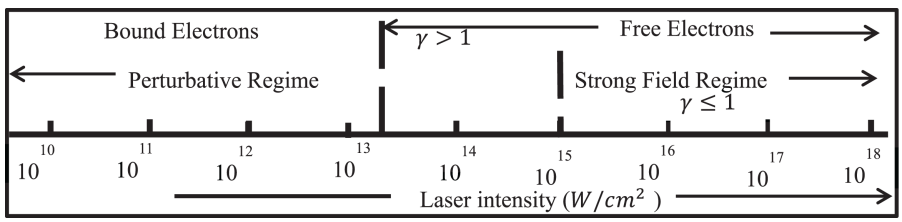

Figure 24.6. Regions of nonlinear optics in terms of the Keldysh parameter (γ) as a function of the incident laser intensity.

This energy, known as ponderomotive energy, is associated with electron oscillation about an equilibrium position. The energy available due to the recombination of photons is the difference between the kinetic energy of the electron and the ionization energy of the atom.

Beyond the perturbative region, a plateau region and a cutoff region for the HHG have been experimentally observed, as described by the following equation:

$$\hbar\omega = I_p + 3.17K. \tag{24.4}$$

Here, I_p is the ionization potential of the atom. The ponderomotive energy or the potential (K) is given by $K \propto I\lambda^2$. Here, I and λ are the laser intensity and the wavelength, respectively. The Keldysh parameter in terms of K is also given by $\frac{1}{\gamma} = \sqrt{\frac{K}{2I_p}}$.

Exercise 24.1. A Ti:sapphire amplifier laser at a wavelength of 800 nm, a pulse duration of 10 fs, and a power output of 10 W at 1 kHz is used in an experiment. The ponderomotive energy for Ar gas is given as 45 eV. For a laser pulse beam spot of 1 mm, how many harmonics are generated? The given value of the Ar ionization potential is 15.8 eV.

Solution. We can find the peak power (W cm^{-2}). However, for the given data and using equation (24.4), we can obtain the cutoff energy of the harmonic, which is 158.45 eV. Dividing this value by the corresponding energy of the pump wavelength (800 nm) we obtain the harmonic number, which is 92. (For details, see [16].)

The experimental scheme for HHG using tunnel ionization is shown in figure 24.7. Here, a high-intensity laser beam is focused on a jet stream of a gas, generating high harmonics as indicated in figure 24.8. The intensity of the laser beam can be as large as ($10^{18} \sim 10^{20}$ cm^{-2}), which allows a large number (i.e. a few hundred) of odd harmonics to be obtained.

There are three regimes in the observed HHG spectrum: (i) the perturbative region, (ii) the plateau region and (iii) the cutoff region. It should be noted that the intensities of the various orders of higher harmonics are of the same order of magnitude in the plateau region (figure 24.8). There is a cutoff value below which HHG is not obtained. For example, in figure 24.8, the cutoff is approximately near the 28th harmonic.

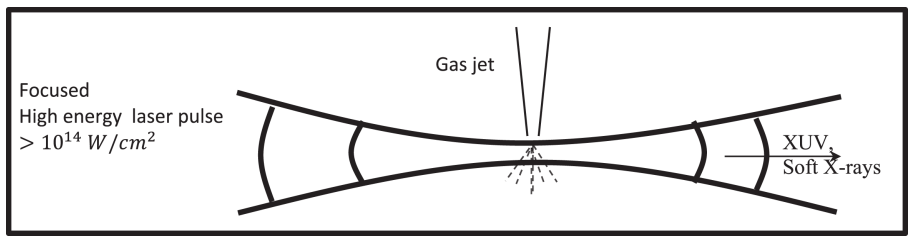

Figure 24.7. An experimental scheme for high harmonic/soft x-ray generation.

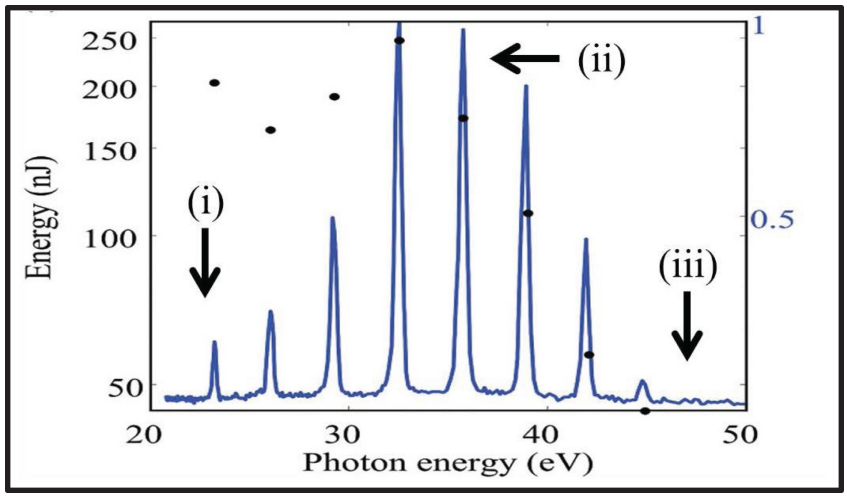

Figure 24.8. Typical HHG spectrum obtained from argon gas pumped by a femtosecond laser. The pulse energy per individual harmonic is indicated by dots (reprinted from [10] with the permission of AIP Publishing). The perturbative region (i), the plateau region (ii), and the cutoff region (iii) are also indicated.

24.2.2.2 Odd harmonics in HHG

The symmetry properties of centrosymmetric materials, such as liquid and gaseous media (♠ see chapter 16), are especially important to our understanding of the observed behavior. It should be noted that for centrosymmetric systems, only odd harmonics can be obtained, as $\chi^{(2)}$ is zero. However, for non-centrosymmetric systems, both odd and even harmonics are obtained.

24.2.2.3 Tunnel ionization model of HHG

Ultrafast femtosecond laser pulses carry the electric field required for the generation of high harmonics. Due to the inverse square law dependence of the coulomb potential, the electron feels an appreciable force in the field of the incident laser pulse. Since the nucleus is heavy compared to electrons, the electrons are accelerated very close to the nucleus. Due to the oscillatory nature of the incident optical field, the electrons approach the nucleus during each period, as shown in figure 24.9(A). This process modifies the potential well, facilitating electron tunneling as shown in figure 24.9(B). The frequency of the radiation emitted during the recombination process is proportional to the incident field acceleration and its optical period. This model, known as the *tunnel ionization model*, is used to explain the generation of high harmonics. It is summarized as follows:

1. An atom irradiated by the strong laser field of a laser pulse can be ionized into a parent ion and a free electron with no initial kinetic energy.
2. The electric field of the laser accelerates the electron.
3. When the electron collides with the parent ion, the ion and electron can recombine. The total extra energy (i.e. the kinetic energy of the electron plus the binding energy of the atom, *Ip*) is released by the emission of a photon of a higher harmonic.

24.2.2.4 Sub-femtosecond-duration pulse generation

In the HHG process, a sequence of pulses is produced within a short-duration femtosecond pump pulse. A train of higher harmonic pulses is obtained; these pulses are of even shorter (i.e. sub-femtosecond or attosecond (10^{-18} s)) duration, as shown in figure 24.10. In a collection of atoms, the maximum number of electrons is ejected at the positive or the negative half cycles of the optical pulse. Therefore, the sequence of pulses is generated at double the repetition rate of the fundamental pulse. In the cascaded Raman process, however, the Fourier transform of the

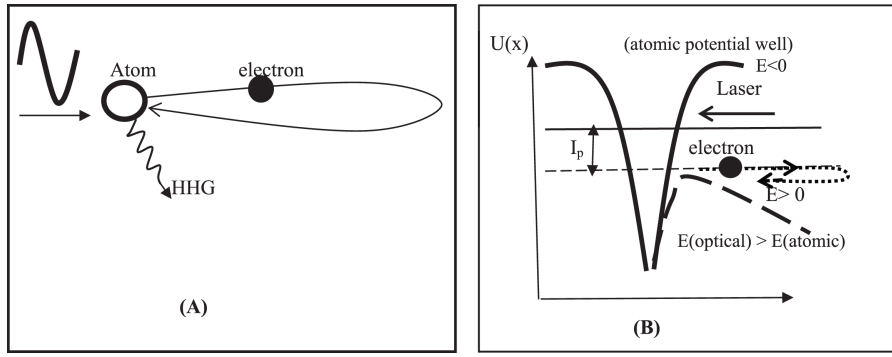

Figure 24.9. Mechanism of HHG: in an optical cycle of a laser pulse, an electron from an ionized atom is accelerated and recombined (A). The modification of the potential well that occurs when the intense laser beam strikes the material is shown in (B).

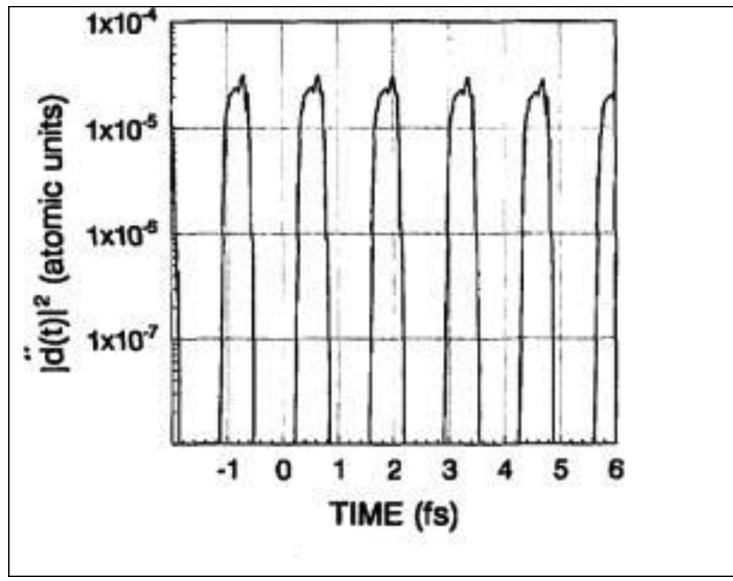

Figure 24.10. Attosecond-duration pulses produced by HHG in neon, seen in the temporal domain. (Reproduced with permission from [9], copyright The Optical Society.)

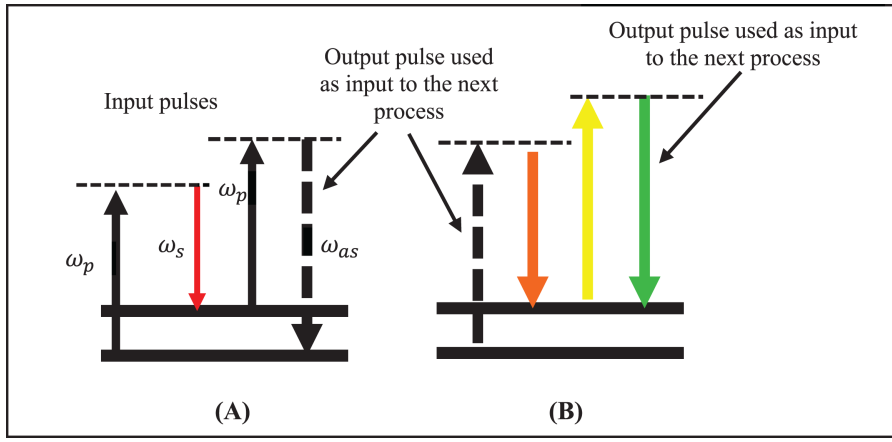

Figure 24.11. High harmonics generated by the stimulated Raman scattering process: the anti-Stokes frequency of the first Raman process (A) acts as the pump pulse of the second process (B), and so on. ω_p, ω_s, and ω_{as} are the pump, Stokes, and anti-Stokes frequencies, respectively.

sidebands gives rise to pulses at the same repetition rate, as described in the following section.

24.2.2.5 Cascading Raman effect

The concept of the Raman effect was introduced in chapter 16 (section 16.8). In the sequential or cascaded Raman process, two lasers are used, one of which is tunable in frequency. For example, a Nd:YAG laser (with frequency of ω_p) along with a tunable Ti:sapphire laser can be used in such a way that the tunable frequency difference is equal to the fundamental vibrational frequency ($\Delta\omega_v$) of the molecular system.

In the first state of the process, due to stimulated Raman scattering (SRS), the input pulses give rise to an output anti-Stokes pulse. In the subsequent Raman process, this output pulse is used as the input pulse, as shown in figure 24.11. At high intensity, for two input frequencies that are nearly resonant with a Raman resonance, the process cascades several times, yielding a series of equally spaced modes according to $\Delta\omega = \omega_p \pm n\Delta\omega_v$, as shown in the image in figure 24.12.

24.3 Present and future outlook

High peak power laser pulses can be generated by the principle of chirped-pulsed optical parametric amplification (CPOPA). When this is combined with the techniques of HHG in the soft x-ray and EUV regions, pulse lengths on timescale of the hundreds of attoseconds can be obtained. These pulse durations correspond to the order of the revolution time of an electron in the first Bohr orbit of the hydrogen atom.

♣ Part of the Noble prize was awarded to Strickland and Mourou in 2018 for inventing the CPOPA technique. The other part was awarded to Arthur Ashkin for the optical trapping of particles.

♣ In hydrogen, electron completes a revolution in its orbit in ~124 as.

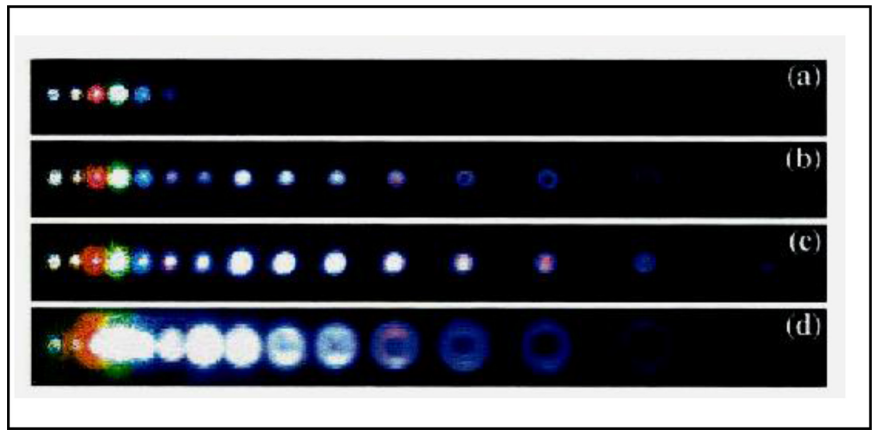

Figure 24.12. Raman frequency spots produced by the cascaded Raman process: (a) to (c) at 70 Torr, (d) is at 350 Torr of pressure. The first two spots are the driving frequencies of the Nd:YAG and Ti:sapphire lasers attenuated by several orders. Reprinted (Fig. 2) with permission from [11], copyright (2000) by the American Physical Society.

Gas-filled capillary waveguides are phase matched to obtain high harmonics. It should be mentioned that the durations of attosecond pulses can also be measured using the same principle as those of the pump-probe autocorrelation techniques described in chapter 18. In these regions, the autocorrelation techniques are known as the *reconstruction of attosecond beating by interference of two-photon transitions* (RABBIT) and *frequency-resolved optical gating for complete reconstruction of attosecond bursts* (FROG-CRAB)[1].

The future of laser physics and photonics continues to be interesting and highly promising, as can be seen from the application areas of high-power laser research summarized in figure 24.13 by Mourou and Tajima. The figure shows the inverse linear dependence between the pulse duration of coherent light emission and the obtained laser intensity for more than 18 orders of magnitude .

Questions and problems

1. Name a few laser gain media consisting of transition metals or rare-earth ions as constituents in a host system.
2. A laser cavity typically has two mirrors. What is the principle of the 'mirrorless laser'?
3. The cyclotron is a particle accelerator. What are the major differences between the synchrotron, the cyclotron, and the free-electron laser?
4. You must have done experiments using a Michelson interferometer in undergraduate laboratory classes. The Michelson interferometer is also used to detect gravitational waves at the Laser Interferometric Gravitational-Wave Observatory (LIGO). In the LIGO, why are the arm lengths of the Michelson interferometer several kilometers long?

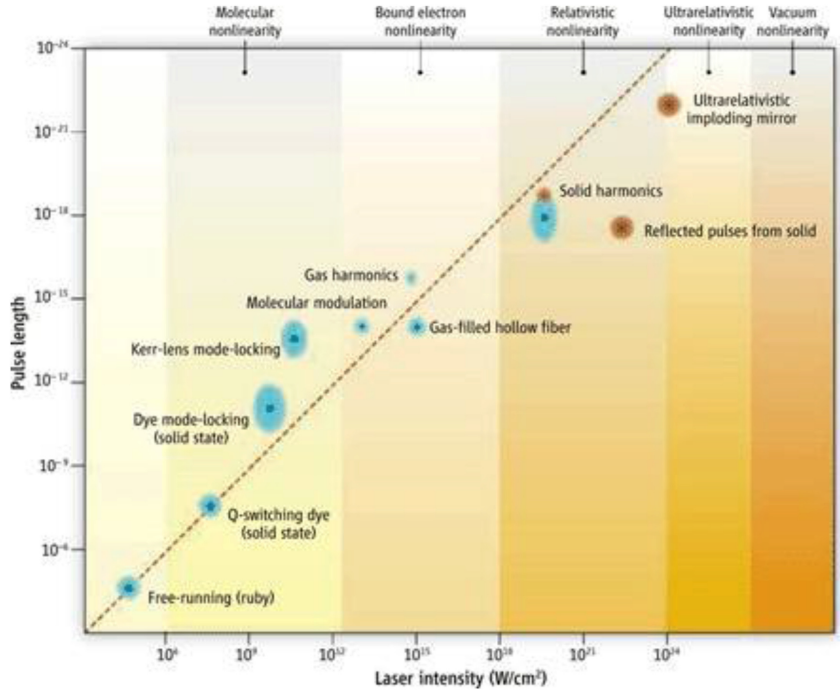

Figure 24.13. Phenomena that are accessible with the development of short-duration intense pulses (from [15], reprinted with permission from AAAS).

5. In the FEL, electrons are accelerated to relativistic speeds. Describe the mechanism that allows FELs to obtain a large degree of frequency tunability from the UV to millimeter regions.
6. Obtain the expression for the time-averaged kinetic energy (i.e. the ponderomotive energy) associated with the motion of a free electron (of charge e and mass m) in an electric field E whose frequency ω given by $E = E_0 e^{-i\omega t}$.
7. The cutoff frequency for HHG is given by equation (24.4). For a particular system, the ponderomotive energy is given in eV by $K = 9.33 \times 10^{-14} I_L\ (\text{W cm}^{-2})\lambda_L^2(\mu\text{m}^2)$. A typical experiment uses a Ti:sapphire laser at a wavelength of 800 nm, a pulse duration of 33 fs, and an output power of 6 W at 1 kHz. If the laser pulse has a focused spot size of 2 mm in He gas inside a capillary, estimate the number of harmonics generated. Take the ionization potential of He to be 24.6 eV. (♠ Also see [16].)
8. What is the three-step model of high harmonic generation? Under what conditions are only the odd harmonics generated?
9. How does the *stimulated* Raman scattering from a material contribute to the generation of new frequencies?
10. What is the mechanism by which high harmonics are generated using the cascaded Raman effect?

Bibliography

[1] Kogelnik H and Shank C V 1972 Coupled-wave theory of distributed feedback lasers *J. Appl. Phys.* **43** 2327–35

[2] Scifres D R, Burnham R D and Streifer W 1974 Distributed-feedback single heterojunction GaAs diode laser *Appl. Phys. Lett.* **25** 203–6

[3] Sailaja R and Bisht P B 2007 Tunable multiline distributed feedback dye laser based on the phenomenon of excitation energy transfer *Org. Electron. physics, Mater. Appl.* **8** 175–83

[4] Huang S *et al* 2017 Dual-cavity feedback assisted DFB narrow linewidth laser *Sci. Rep.* **7** 1185

[5] Attwood D S 1999 *X-Rays and Extreme Ultraviolet Radiation: Principles and Applications* (Cambridge: Cambridge University Press)

[6] Popov V S 2004 Tunnel and multiphoton ionization of atoms and ions in a strong laser field (Keldysh theory) *Phys. Usp.* **47** 855

[7] Augst S, Strickland D, Meyerhofer D D, Chin S L and Eberly J H 1989 Tunneling ionization of noble gases in a high-intensity laser field *Phys. Rev. Lett.* **63** 2212–5

[8] Corkum P B 1993 Plasma perspective on strong field multiphoton ionization *Phys. Rev. Lett.* **71** 1994–7

[9] Corkum P B, Burnett N H and Ivanov M Y 1994 Subfemtosecond pulses *Opt. Lett.* **19** 1870–2

[10] Rudawski P *et al* 2013 A high-flux high-order harmonic source *Rev. Sci. Instrum.* **84** 73103

[11] Sokolov A V, Walker D R, Yavuz D D, Yin G Y and Harris S E 2000 Raman generation by phased and antiphased molecular states *Phys. Rev. Lett.* **85** 562–5

[12] Strickland D and Mourou G 1985 Compression of amplified chirped optical pulses *Opt. Commun.* **56** 219–21

[13] Durfee C G *et al* 1999 Phase matching of high-order harmonics in hollow waveguides *Phys. Rev. Lett.* **83** 2187–90

[14] Trebino R 2000 *Frequency-Resolved Optical Gating: The Measurement of Ultrashort Laser Pulses* (New York: Academic)

[15] Mourou G and Tajima T M 2011 Intense, shorter pulses *Science (80–)* **331** 41 LP–2

[16] Gibson E A *et al* 2004 High-order harmonic generation up to 250 eV from highly ionized argon *Phys. Rev. Lett.* **92** 33001